ACS OMEGA

Open Access

http://pubs.acs.org/journal/acsodf

Article

Origin of Long-Range Hyperfine Couplings in the EPR Spectra of 2,2,5,5-Tetraethylpyrrolidine-1-oxyls

Yuliya F. Polienko,* Sergey A. Dobrynin, Konstantin A. Lomanovich, Anastasiya O. Brovko, Elena G. Bagryanskaya, and Igor A. Kirilyuk

Cite This: *ACS Omega* 2023, 8, 38723−38732

Read Online

ACCESS | Metrics & More | Article Recommendations | Supporting Information

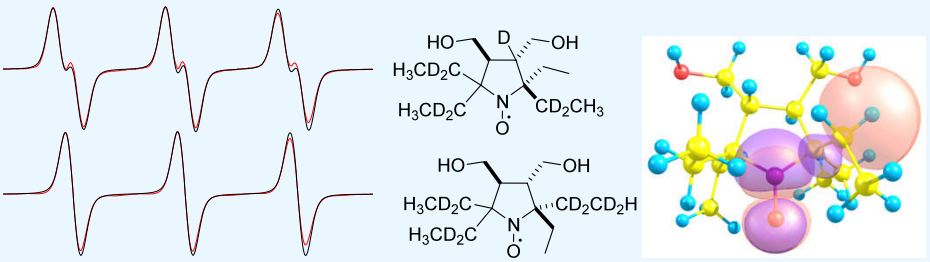

ABSTRACT: Cyclic nitroxides with several bulky alkyl substituents adjacent to the nitroxide group are known to demonstrate a much higher stability to bioreduction than their tetramethyl analogues. Among these so-called "sterically shielded" nitroxides, the pyrrolidine derivatives are the most stable. The EPR spectra of some sterically shielded pyrrolidine-1-oxyls were reported to show one or two large additional doublet splittings with a hyperfine coupling (hfc) constant (ca. 0.2−0.4 mT). To determine the origin of these hfc, a series of 2-*R*-2,5,5-triethyl-3,4-bis(hydroxymethyl)-pyrrolidine-1-oxyls with methylene groups stereospecifically enriched with deuterium were prepared, and their CW EPR spectra were studied. In addition, these nitroxides were investigated using quantum chemical calculations on the UB3LYP/def2-TZVP level and NBO analysis. The apparent constants were assigned to hfc with γ-hydrogen in the side chain, with the contribution of the NBO orbital $^{\beta}\pi^{*}$(N−O) to the natural localized molecular orbital $^{\beta}\sigma$(C−H) playing the major role. This interaction is efficient if the ethyl substituent is in the pseudoaxial position of the ring and the CH_2−CH_3 bond is codirected with (parallel to) N−O. The apparent constant a_H increases with the Boltzmann population of this conformation.

INTRODUCTION

Nitroxides have found plenty of applications in various fields of science and technology.[1−3] A broad majority of commonly used nitroxides have a cyclic structure with four methyl substituents adjacent to the N−O group. Recently, nitroxides with bulkier alkyl substituents, e.g., ethyls, instead of methyls attracted much attention. These so-called "sterically shielded" nitroxides demonstrate a much higher stability against chemical reduction to diamagnetic compounds with components of biological systems than their tetramethyl analogues.[4−6] To date, sterically shielded pyrrolidine-1-oxyls demonstrate the highest resistance to reduction among all known nitroxides.[7−9] They also demonstrate relatively high stability to oxidative destruction in the presence of rat liver microsomes.[10] The EPR spectra of some of these nitroxides, e.g., structures **1a−c** and **2** (Figure 1), reveal one or two large additional doublet splittings with a hyperfine coupling (hfc) constant (ca. 0.2−0.33 mT).[7,9,11] Similar spectral features were earlier observed for some cyclic nitroxides with a five-membered saturated ring and bulky substituents adjacent to the N−O· group, i.e., oxazolidine **3**[12,13] and imidazolidine **4**[14] nitroxides (Figure 1). To the best of our knowledge, a large hfc was never observed in the EPR spectra of conventional tetramethyl nitroxides.

To assign the splittings in the EPR spectra of **3** and **4**, their partially deuterated analogues were used. Replacement of four methylene hydrogens to deuterium in geminal ethyl groups in position 2 or 5 in **4** or in methylene groups next to the spiro node in the cycloalkane ring in **3** resulted in the disappearance of additional splitting,[13,14] unambiguously showing that the unpaired electron has a large hfc with one of the γ-hydrogens in the side chain. This assignment for **4** was supported by the UB3LYP/def2-TZVP level DFT calculations. Large couplings reflect the difference between the Boltzmann populations of different conformations. The calculations predicted only one large a_H constant per pair of geminal ethyl groups for all low-energy conformers, assuming that all of these conformers

Received: August 17, 2023
Accepted: September 8, 2023
Published: October 9, 2023

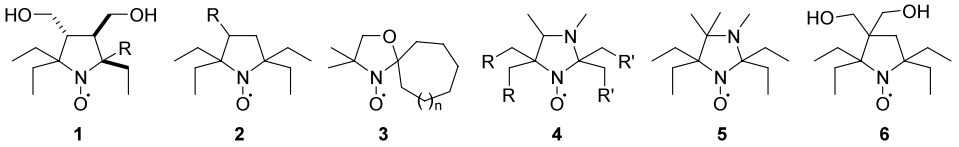

1: R = Et (**a**), i-Pr (**b**), t-Bu (**c**). **2**: R = COOX, CH_2Y. **3**: n = 4,5,8. **4**: R =H (**a**), Me (**b,c**), R' = Me (**a,c**), H (**b**).

Figure 1. Structures of nitroxides **1**−**6**.

Scheme 1. Synthesis of Nitrones 8a,b (in Analogy to Ref 7)

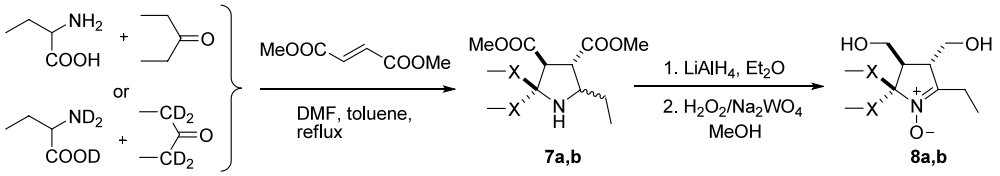

7,8: X = CH_2 (**a**); CD_2 (**b**).

Scheme 2. H-D Exchange in 8a,b

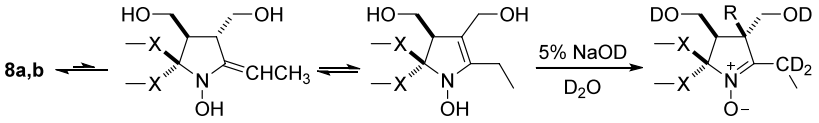

8: X = CH_2 (**a,c**); CD_2 (**b,d**). R = H (**a,b**), D (**c,d**).

contribute to the apparent average hfc constant. This result did not allow to assign the large constants neither to a definite atom(s) nor to definite ethyl group(s). Recently, another pattern of the hyperfine structure was described for newly synthesized sterically shielded nitroxides **5** and **6** with only one large splitting of ca. 0.38−0.40 mT on a hydrogen atom.[11,15]

Complicated hyperfine structure and line broadening in the EPR spectra of sterically shielded nitroxides makes them inefficient in EPRI and OMRI applications, where radicals with a minimal number of narrow lines are required for better resolution and enhancement.[16−18] Broadened spectral lines can also hamper analysis of molecular dynamics using spin labeling and EPR.[6] A better understanding of the factors affecting the hyperfine structure in the EPR spectra of sterically shielded nitroxides could help in the molecular design of better structures.

The original method we used for the preparation of various sterically shielded nitroxides, such as **1**, **2**, **5**, and **6**, implies the addition of ethynylmagnesium bromide to corresponding cyclic nitrone with the subsequent hydrogenation of the terminal acetylene group.[9,11,15] This method perfectly fits for the preparation of 3,4-bis(hydroxymethyl)-2,2,5,5-tetraethylpyrrolidine-1-oxyls with varying numbers and positions of deuterium atoms. A set of partly deuterated analogues of **1a** were prepared. The CW EPR spectra of these nitroxides and the corresponding ethynyl-substituted precursors were investigated. DFT calculations were performed for **1a**−**c** and **5** and the obtained canonical orbitals were analyzed using the NBO method to reveal the relationship between the structure and the observed hfc constants.

RESULTS AND DISCUSSION

Synthesis. The synthesis of 2,2,5-triethylpyrrolidine **7a** (stereoisomeric mixture) from 2-aminobutanoic acid, diethyl ketone, and dimethyl fumarate and its conversion into nitrone **8a** was described earlier[7] (Scheme 1). The isotope-labeled compound **7b** was prepared from 3-pentanone-(2,4-D_2). To prevent reverse exchange of deuterium for protium, mobile protons in 2-aminobutanoic acid were replaced for deuterium via iterative dissolution in D_2O evaporation procedures. The solvent mixture (DMF−toluene) was heated to reflux with D_2O in the Dean−Stark apparatus prior to the use in the synthesis of **7b**.

Reduction of the diastereomeric mixture **7b** with $LiAlH_4$ followed by oxidation with H_2O_2/Na_2WO_4 afforded nitrone **8b** (Scheme 1). α-Alkylnitrones are known to demonstrate significant CH acidity and nitrone-ene-*N*-hydroxyamine tautomerism.[19] Proton exchange in the alkaline solution of **8a,b** was used to replace methylene hydrogens of the 2-ethyl substituent and hydrogen atom in position 3 of the heterocycle by deuterium (Scheme 2). The rate of exchange was remarkably different for these three hydrogens. For example, the intensity of the signals of diastereotopic methylene hydrogens in the ^1H NMR spectrum of **8a** in 5% NaOD in D_2O at 20 °C decreased by 95 and 50% on 14 days, while the signal of the hydrogen atom in position 3 of the heterocycle showed a 13% initial intensity (see Figure S4, Supporting Information). The difference in the H-D exchange rates for diastereotopic protons is a well-known phenomenon (see, e.g., ref 20). The exchange procedures were finished after the enrichment of the methylene group at the nitrone carbon with D reaching 95% in **8c,d**.

We reported earlier that nitrone **8a** can form an insoluble precipitate upon treatment with the Grignard reagent in THF, and this may impede addition to nitrone.[7] To prevent the precipitate formation, the hydroxymethyl groups were protected with 2,2-dimethoxypropane. The addition of ethynylmagnesium bromide to 5-*R*-2,2-diethyl-3,4-bis(((2-methoxypropan-2-yl)oxy)methyl)-3,4-dihydro-2*H*-pyrrole 1-oxides (**9a**−**c**) was shown to afford a single isomer (racemate)

https://doi.org/10.1021/acsomega.3c06090
ACS Omega 2023, 8, 38723−38732

with the ethynyl group in the cis-position to the neighboring hydroxymethyl group, and the structures of the corresponding nitroxides **10a–c** were confirmed by single-crystal X-ray analysis data[11] (Scheme 3). Here, we used trimethylsilyl

Scheme 3. Synthesis of Nitroxides 10a and 12a–c

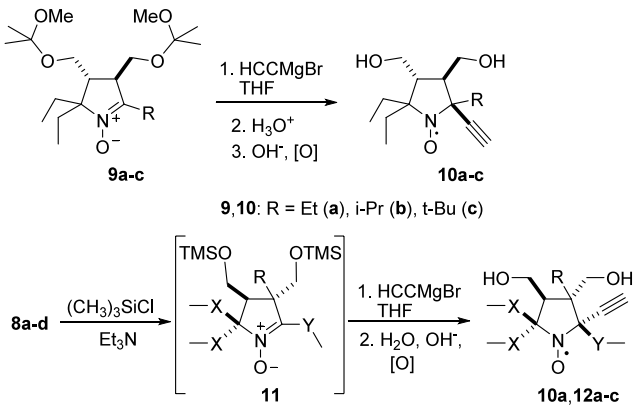

chloride to protect the hydroxymethyl groups in nitrones **8a–d**. The resulting crude nitrones **11** without purification were treated with ethynylmagnesium bromide. Subsequent quenching and oxidation with air oxygen in the alkaline solution of methylene blue in analogy to the previously reported procedure[11] afforded nitroxides **10a** and **12a–c**. The ^{1}H NMR spectrum of the **10a** sample prepared using TMS protection (see Figure S8, Supporting Information) showed no trace of other isomers and corresponded to the previously published data.[11]

Nitroxides **10a** and **12a–c** were subjected to hydrogenation on Pd/C using $^{1}H_2$ or $^{2}H_2$. Subsequent oxidation with air oxygen gave nitroxides **13a–d** and **14**, differing in the number and position of deuterium atoms in the molecule (Scheme 4).

EPR Studies. In the hyperfine structure of the isotropic EPR spectrum of a nitroxide, a splitting on the nitroxide nitrogen (a triplet for ^{14}N) is usually complemented with additional couplings with other magnetic nuclei, e.g., hydrogens. The coupling constants a_H may be positive or negative depending on the nitroxide structure and conformation. In a broad majority of nitroxides, fast conformational motions lead to dynamic averaging of hydrogen hyperfine couplings, making the resulting a_H small. As a result, multiple unresolved lines in the EPR spectra of conventional nitroxides are usually represented as inhomogeneously broadened triplet. If a conformation with high a_H prevails, e.g., due to steric interactions in the molecule, the resulting Boltzmann average a_H may be high enough to produce a significant visible splitting of the nitroxide triplet spectral lines. Examples of such behavior are given in the introduction. The deuterium nucleus has a higher nuclear spin (s = 1) but 6.5-fold lower hfc constant than ^{1}H. The partial deuteration of nitroxides **3** and **4** was previously used to suppress large splitting on the ^{1}H nucleus ($a_H \approx 0.2$ mT) in the EPR spectra because smaller triplet splitting $a_D \approx 0.03$ mT was no longer resolved and only contributed to the apparent line width.

The EPR spectra of nitroxides **1a**, **10a**, **12a–c**, **13a–d**, and **14** are shown in Figure 2, and the parameters of the spectra are listed in Table 1. The hyperfine structure of the spectra of the nitroxides shows clear dependence on the amount and position of ^{1}H and ^{2}H atoms in the structure. In general, it follows the pattern previously described for **4**:[14] each pair of geminal ethyls adjacent to the nitroxide group can produce one additional large splitting. Replacement of all methylene hydrogens in geminal pairs of ethyls for deuterium suppresses the apparent large splitting (cf. **1a** and **13b,d**), but the lines remain inhomogeneously broadened because the unresolved hfc with deuterium contributes to the line widths. In our previous investigation, neither the experimental data nor high-level DFT calculations allowed assignment of the large a_H in the EPR spectra of **4a–c** to a specific ethyl group of the geminal pair because low conformational barriers implied fast exchange between the conformations (ethyl group rotation and ring puckering).[14] The above procedure of the synthesis of nitroxides **12**, **13**, and **14** afforded stereospecifically deuterated compounds, and this gives an opportunity to separate the influence of hydrogen atoms in different positions of the molecule on the hyperfine structure of the EPR spectrum. The spectra of partly deuterated nitroxides **13c** and **13d** are nearly identical triplets with minor differences in the line widths. In contrast, the spectrum of **14** shows additional splitting, a_H = 0.23 mT. Therefore, replacement of ^{1}H for ^{2}H in the methylene moiety of the ethyl group trans to the neighboring hydroxymethyl one produces a negligible effect, while protons of the cis-ethyl group show a large hfc. Obviously, even if the conformational barriers are low, a hydroxymethyl group at the asymmetric center at position 3 of the ring brings strong asymmetry to the population of the conformations of neighboring ethyl groups. This feature makes nitroxide **1a** fundamentally different from **3**, **5**, and **6**, where conformations are degenerate and protons of both geminal substituents may equally contribute to the apparent large constant. As a practical consequence, it is sufficient to replace the protons of one particular methylene group in each geminal ethyl pair in **1a** to remove the large splitting on γ-hydrogens in the EPR spectrum.

Comparison of the EPR spectra of various sterically shielded nitroxides with a five-membered saturated ring (see, e.g., refs 11 and 15) shows that the value of a_H may vary over a wide range, varying with minor structural changes. For example, in **1a–c**, the increase of the substituent R by one methyl group leads to the growth of one of the two a_H from 0.224 to 0.331 mT (R = *i*-Pr), but the addition of one more methyl group (R

Scheme 4. Synthesis of Nitroxides 13a–d and 14

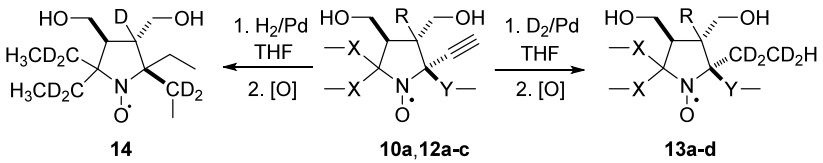

https://doi.org/10.1021/acsomega.3c06090
ACS Omega 2023, 8, 38723–38732

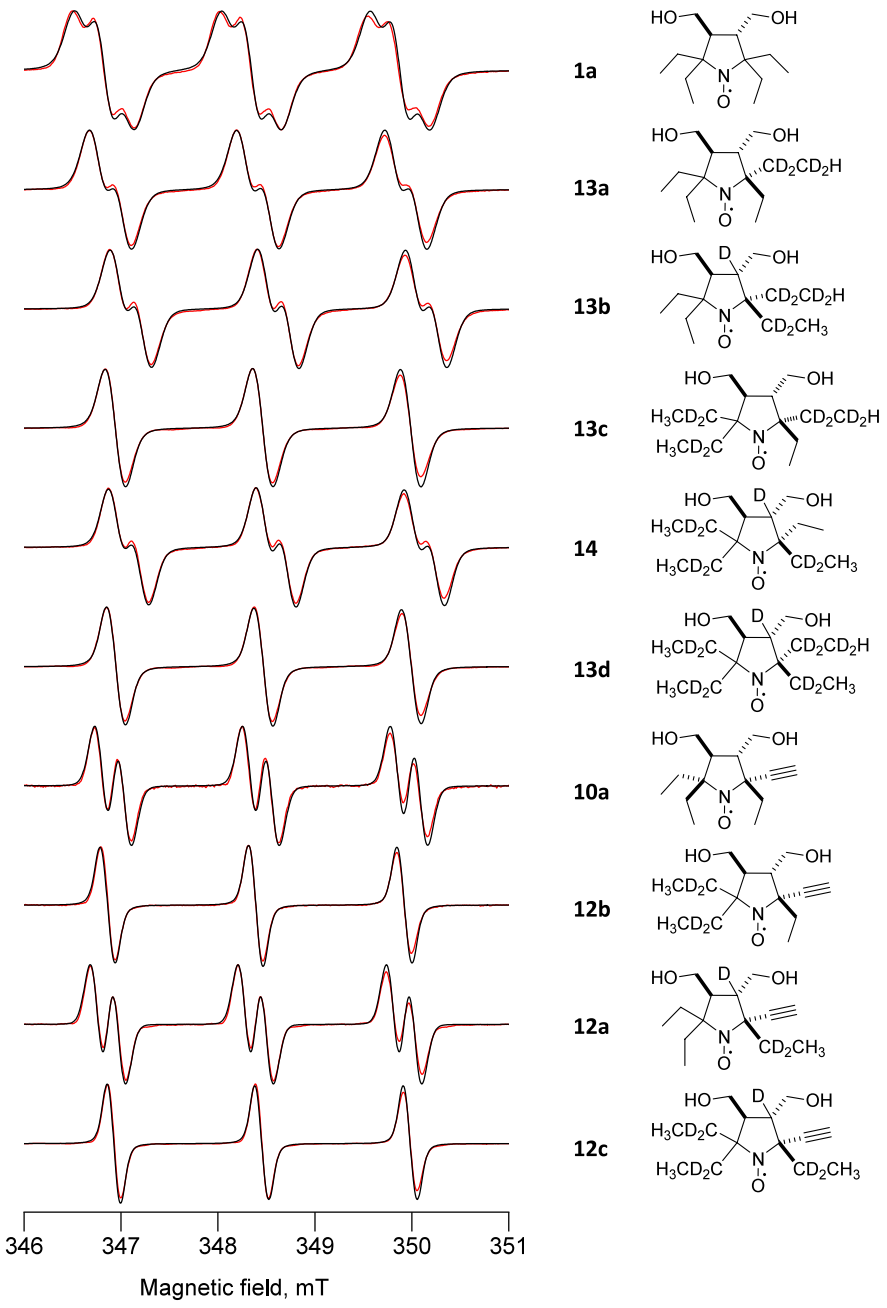

Figure 2. Experimental (red) and calculated (black) EPR spectra of nitroxide shown on the right side. The parameters of simulation are listed in Table 1.

Table 1. Parameters of the EPR Spectra and Simulations

					line width	
no.	g	a_N (mT)	a_1 (mT)	a_2 (mT)	Gauss (mT)	Lorenz (mT)
1a	$2.0057 \pm 5 \times 10^{-5}$	$1.53 \pm 2 \times 10^{-3}$	0.23(H)	0.23(H)	0.21	0.05
13a			0.23(H)	0.035(D)	0.19	0.05
13b			0.23(H)	0.035(D)	0.18	0.05
13c			0.035(D)	0.035(D)	0.16	0.05
14			0.035(D)	0.23(H)	0.19	0.03
13d			0.035(D)	0.035(D)	0.14	0.05
10a			0.22(H)		0.16	0.02
12a			0.034(D)		0.12	0.03
12b			0.22(H)		0.14	0.03
12c			0.034(D)		0.13	0.03

https://doi.org/10.1021/acsomega.3c06090
ACS Omega 2023, 8, 38723−38732

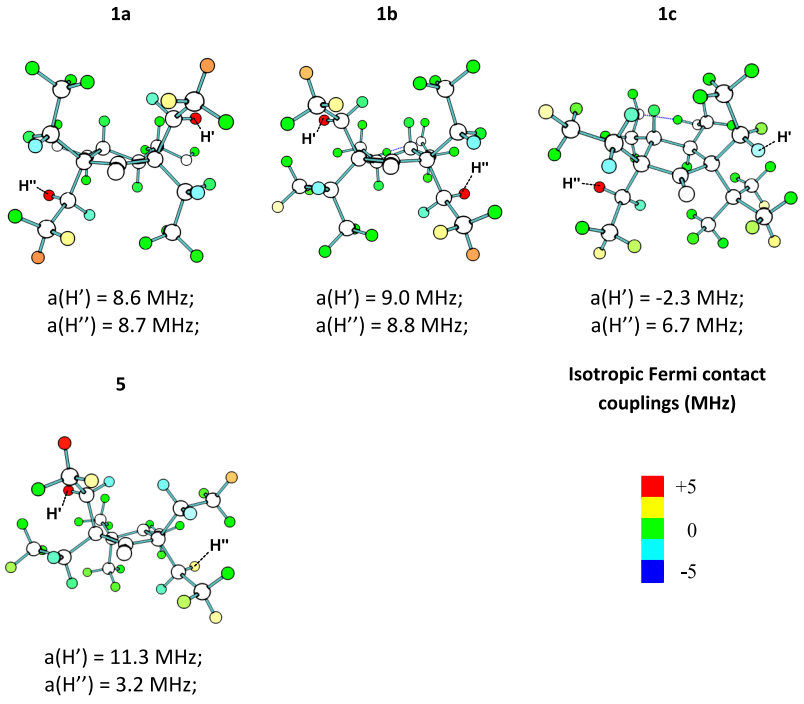

Figure 3. Calculated structures of nitroxides **1a−c** and **5**. The calculated values of isotropic Fermi contact coupling constants are shown with color. The values of the large constants are given in MHz.

= *t*-Bu) results in the disappearance of one of the two a_H.[11] Quantum chemical calculations were used to find the general criteria for the appearance of large hfc splittings and to assign these hfc to specific hydrogen atoms (see below).

Quantum Chemical Calculations. The hfc constants on hydrogens for **1a** (R = Et), **1b** (R = *i*-Pr), **1c** (R = *t*-Bu), and **5** were calculated at the UB3LYP/def2-TZVP level. It is known that special basis sets must be used for the precise prediction of the hfc constant on nitroxide nitrogen ($a_{N(iso)}$) and solvent effects with hydrogen bonding of the nitroxide group must be taken into account. However, these precautions are not needed for the estimation of hfc with hydrogens ($a_{H(iso)}$).[21,22] The observed ^{1}H hfc constants are averaged over the Boltzmann distribution of conformations, and conformations with lower energies have a greater statistical weight. To find the lowest-energy conformations, we used a systematic rotor search method at the MMFF94 level. Since the parameters of the force field for the nitroxide moiety were not available, the parameters for ketones of the same topology were used, whose geometry and electronic properties are very similar. It should be noted that the most favorable conformations found for **1a** and **1c** coincide with the conformations obtained from the X-ray analysis data.[7,11]

The calculated hfc constants on hydrogen atoms for the lowest-energy conformation are shown with color in Figure 3. The hydrogen atoms with the highest a_H are shown in red. The hfc on hydrogens of the methyl group were not taken into account because fast rotation across the CH_2-CH_3 bond should lead to averaging. In agreement with the experimental data, the calculation predicted for **1a** two large isotropic Fermi contact couplings on two ethyl groups in the cis-position to the neighboring hydroxymethyl group. The predicted values of a_H are in good agreement with the experimental data (Table 2). It should be noted that introduction of bulkier substituents (**1b** and **1c**) produces significant changes in the geometry of the molecule. Nevertheless, the structures **1a−c** and **5** demonstrate

Table 2. Predicted and Calculated Values of the Isotropic hfc Constants for Nitroxides 1a−c and 5

nitroxide	atom	$a_{H(iso)}$, MHz/Gauss	$<a_{H(iso)}>$, MHz/Gauss	a_H (experimental), Gauss
1a	H′	8.6/3.1	5.7/2.0	2.24
	H″			2.24
1b	H′	9.0/3.2	8.9/3.2	3.31
	H″	8.8/3.1	6.4/2.3	2.52
1c	H′	−2.3/−0.8	−1.3/−0.5	2.55
	H″	6.7/2.4	6.6/2.4	
5	H′	11.3/4.0	11.2/4.0	3.64
	H″	3.2/1.1	2.3/0.8	

one common feature: the large a_H is predicted on the methylene hydrogen of the ethyl group in pseudoaxial position with the CH_2-CH_3 bond nearly parallel to the N−O axis. This conformation favors overlapping of the smaller lobe of one of the sp^3-hybridized C−H bond orbitals of the methylene moiety of the ethyl group with the nonbonding orbital of the nitroxide group.

To investigate the orbital interactions, NBO analysis was used, which showed a linear dependence of the isotropic constant of the hyperfine interaction on the natural spin density on hydrogen atoms, both within a single molecule and in comparison of molecules **1a−c** and **5** with each other (see the Supporting Information, Figures S37−S41). Interestingly, high values of the hyperfine constants for some hydrogen atoms of methyl groups predicted by UB3LYP/def2-TZVP calculations cannot be explained within the framework of the natural spin density. Presumably, these outliers result from the direct proximity of the hydrogen atoms to the orbitals of the nitroxyl group.

The main process of the emergence of natural spin density on hydrogen atoms can be attributed to the transfer of electronic density from the $^{\beta}\sigma$(C−H) orbital to the $^{\beta}\pi^*$(N−O)

https://doi.org/10.1021/acsomega.3c06090
ACS Omega 2023, 8, 38723−38732

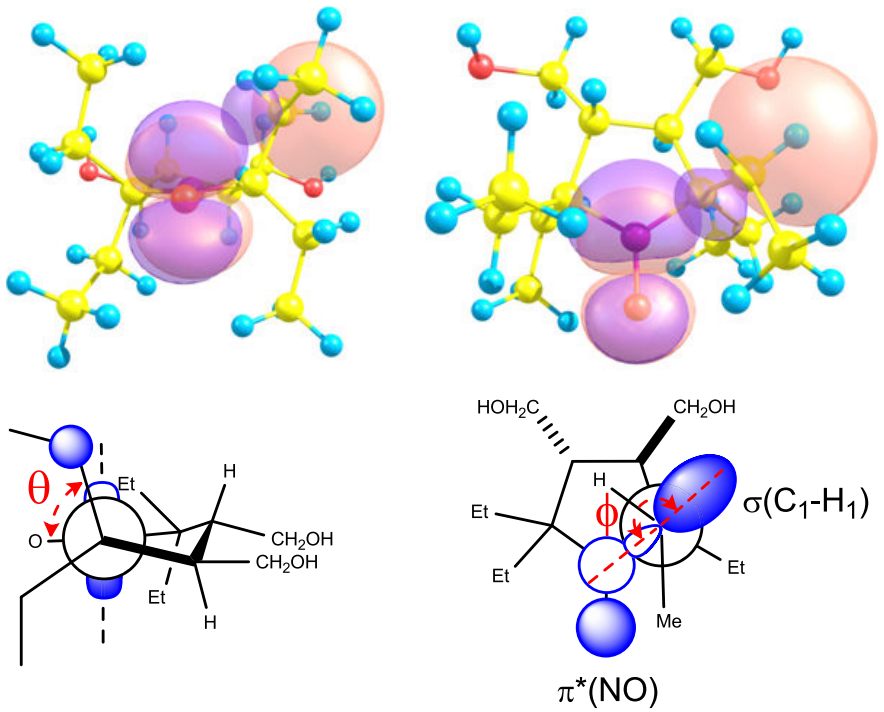

Figure 4. Overlapping of the $^{\beta}\sigma$(C−H) and $^{\beta}\pi^{*}$(N−O) orbitals and dihedral angles φ (N−C−C−H′) and θ (O−N−C−C).

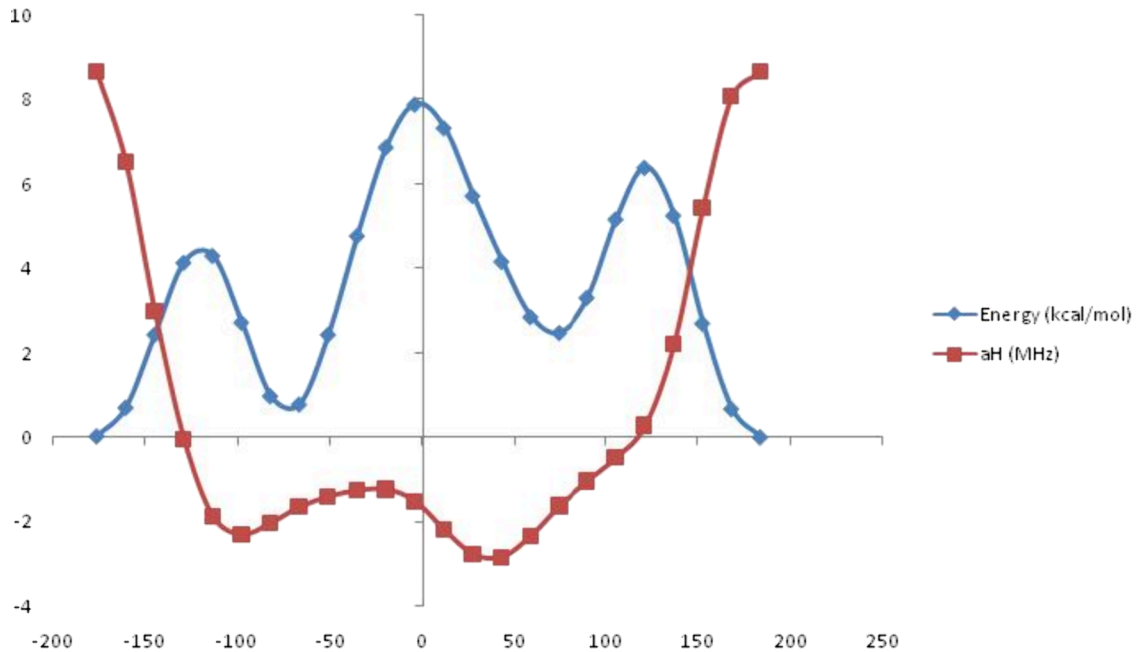

Figure 5. Relaxed scanning of the dihedral angle φ (N−C−C−H′) for nitroxide **1a**.

orbital in the β-spin space due to their direct overlap. Another large transfer of electronic density is observed from the $^{\alpha}$n(N) orbital to the $^{\alpha}\sigma^{*}$(C−H) orbital in the α-spin space, and it should be noted that both effects contribute to an increase in the difference in the α and β populations of the hydrogen atoms. This is clearly demonstrated by the decomposition of natural localized molecular orbitals on the basis of natural bond orbitals (see the Supporting Information, Table S2). In the series of nitroxides, a linear dependence is observed between a_{H} and the contribution of the NBO orbital $^{\beta}\pi^{*}$(N−O) to the natural localized molecular orbital $^{\beta}\sigma$(C−H) (see the Supporting Information, Figure S42).

The above mechanism of the emergence of spin density on hydrogen atoms should be highly sensitive to changes in the geometry of the molecule, mainly on dihedral angles φ (N−C−C−H′) and θ (O−N−C−C) (Figure 4).

Relaxed scanning of the dihedral angle φ (N−C−C−H′) was performed for nitroxides **1a**−**c** and **5** (Figure 5 and Supporting Information, Figures S43−S49). The comparison of the graphs for **1a**, **1b**, and **1c** shows that the conformation with the minimal energy does not always correspond to the

https://doi.org/10.1021/acsomega.3c06090
ACS Omega 2023, 8, 38723−38732

highest a_H. Moreover, the value of a_H depends not only on the steric demand but also on the shape of the substituent.

Boltzmann averaging of the isotropic $a_{(iso)H}$ constants over the rotation of the ethyl group certainly does not provide a complete account of the entire conformational ensemble, but it gives a qualitative representation. For instance, in the case of **1a** and **1b**, averaging over rotation at 298 K leads to a decrease in the average values of $\langle a_{H'(iso)}\rangle$, while in the case of **1c**, it practically disappears. The initial $a_{H(iso)}$ and averaged data $\langle a_{H(iso)}\rangle$ are listed in Table 2.

The estimated values of hfc constants $\langle a_{(iso)H}\rangle$ expectedly differ from experimental data a_H, but they adequately reflect the experimentally observed trends for nitroxides of both imidazolidine and pyrrolidine series. The emergence of the large a_H seems to be a general phenomenon for nitroxides with a five-membered saturated ring and large alkyl substituents adjacent to the N−O group. The large a_H should be attributed to γ-hydrogen in the side chain, for which the σ-orbital of the C−H bond overlaps with the nonbonding orbital of the nitroxide group. The apparent a_H is high if a conformation where such an overlapping occurs is predominant.

CONCLUSIONS

In this work, we studied the origin of the large additional hfc constants in the EPR spectra of some nitroxides with a five-membered saturated ring. The a_H of 0.15−0.4 mT were observed in the spectra of some sterically shielded nitroxides with large alkyl substituents adjacent to the N−O group. Some of these nitroxides demonstrate high resistance to bioreduction, but the complex structure of their EPR spectra makes their use in a number of applications unfavorable. The large hfc constants were found to result from overlapping of the smaller lobe of the C−H orbital in the α-position of the side alkyl chain and the nonbonding orbital of the nitroxide group. A high Boltzmann population of the conformation, where such an overlapping occurs, is a necessary condition for additional large splitting emergence. Conformational analysis of the nitroxide structure can reveal the hydrogen atoms, which contribute to the a_H, and selective replacement of these hydrogens to deuterium can suppress the undesired splitting.

Satisfactory prediction of the hfc constant value can be achieved via Boltzmann averaging over the rotation of the ethyl (alkyl) group in a low-energy conformation. These predictions can help in the molecular design of the new structures with desired properties. Minor structural changes may change the Boltzmann population of conformations and produce significant changes of a_H. The possibility of creating functional spin probes based on this principle deserves further study.

EXPERIMENTAL SECTION

Compounds **1a−c**, **10a**, and **5** were prepared according to the literature protocols.[11] The ^{1}H NMR spectra were recorded at 300, 400, or 500 MHz as indicated next to each NMR analysis. The NMR spectra of nitroxides were recorded from their amines formed under reduction by the Zn/TFA system: to the solution of the nitroxide (15 mg) in CD_3OD (250 μL), Zn powder (100 mg) was added, and the resulting mixture was heated to gentle reflux under stirring. After that, TFA (100 μL) was added dropwise, and the mixture was heated under stirring maintaining the reflux (15 min), filtered into an NMR tube, and diluted to the required volume with $CDCl_3$ or acetone-d_6. The IR spectra were acquired on an FT-IR spectrometer in KBr or neat (for oils) and are reported in wavenumbers (cm^{-1}). The HRMS spectra were recorded on a double-focusing, high-resolution mass spectrometer equipped with high-performance toroidal ESA. Reactions were monitored by TLC carried out using UV light 254 nm, 1% aqueous permanganate, and 10% solution of phosphomolibdic acid in ethanol and/or Dragendorff's reagent as visualizing agents. Column chromatography was performed on silica gel 60 (230−400 mesh).

Dimethyl 2,2-Di(1-$^2H_4$)ethyl-5-ethyl-3,4-pyrrolidinedicarboxylates (7b). To prepare isotope-containing starting materials, 3-pentanone was repeatedly stirred with 5% solution of NaOD in D_2O until methylene proton signals disappeared (2.2%, residual protons; see the Supporting Information, Figure S1) in the ^{1}H NMR spectrum, dried with Na_2CO_3, and distilled; 2-aminobutanoic acid was dissolved in D_2O and solvent was distilled off twice; the mixture of DMF and toluene with D_2O was placed into the Dean−Stark apparatus and stirred under reflux for 4 h. To the mixture of DMF (25 mL) and toluene (25 mL) in the Dean−Stark apparatus, 2-aminobutanoic acid-D_3 (5.3 g, 0.05 mol), dimethyl fumarate (7.2 g, 0.05 mol), and 3-pentanone-D_4 (27 mL, 0.25 mol) were added, and the reaction mixture was stirred under reflux for 45 h (until the amino acid precipitate was completely dissolved). The solvents were distilled off in vacuum, the residue was dissolved in ethyl acetate (100 mL), and the solution was washed with 5% aqueous $NaHCO_3$. H_2O (200 mL) was added, 10% aqueous $NaHSO_4$ solution was added dropwise until the water layer pH = 4, and the organic layer was extracted with 1% aqueous $NaHSO_4$ twice. Acidic extracts were collected and basified with $NaHCO_3$ and extracted with ethyl acetate. The extract was dried with Na_2SO_4, and the solvent was distilled off in vacuum to give 9.42 g (69%) of yellow oil, a mixture of isomers **7b**, which was used for the next step without further purification. IR (neat): ν_{max}: 1733 (C = O). ^{1}H NMR (400 MHz; $CDCl_3$, δ), isomer A (55%): 0.80 (s, 3H), 0.85 (s, 3H), 0.91 (s, 3H), 0.91 (t, J_t = 7.4 Hz, 3H), 1.18−1.31 (m, 1H), 1.46−1.58 (m, 1H), 1.61−1.72 (m, 1H), 2.94 (m, 1H), 3.11−3.19 (m, 2H), 3.63 (s, 3H), 3.64 (s, 3H); isomer B (45%): 0.76 (s, 3H), 0.91 (s, 3H), 0.92 (t, J_t = 7.4 Hz, 3H), 1.31−1.42 (m, 1H), 1.46−1.58 (m, 2H), 3.11−3.19 (m, 1H), 3.24 (dt J_d = 5.3 Hz, J_t = 8.4 Hz, 1H), 3.49 (m, 1H), 3.61 (s, 3H), 3.62 (s, 3H). HRMS (EI/DFS) m/z: $[M]^+$ calcd for $C_{14}H_{21}{}^2H_4NO_4$ 275.2029; found 275.2031.

2,2-Di(1-$^2H_4$)ethyl-5-ethyl-3,4-bis(hydroxymethyl)-3,4-dihydro-2*H*-pyrrole 1-oxide (8b). A solution of crude **7b** (9 g, 0.033 mol) in dry ether (50 mL) was added dropwise to a stirred solution of $LiAlH_4$ (3 g, 0.079 mol) in dry ether (150 mL). The mixture was stirred at ambient temperature for 2 h, and then the flask was placed into a cold water bath and quenched with 10% aqueous KOH. The organic phase was separated via decantation, the remaining wet precipitate was washed with ether 3 × 50 mL, and the combined extracts were evaporated in vacuum. The residue was dissolved in methanol (100 mL) and mixed with a solution of sodium tungstate (1.02 g, 3.2 mmol) and EDTA disodium salt (1.08 g, 3.2 mmol) in water (50 mL) and hydrogen peroxide 30% (17 mL) was added. The solution was allowed to stand at ambient temperature for 24 h, and then a catalytic amount of MnO_2 (0.2 g, 2.3 mmol) was carefully added to quench remaining H_2O_2. After the oxygen evolution ceased, the solution was evaporated in vacuum. The residue was triturated with $CHCl_3$ (30 mL) and Na_2CO_3 (5 g), the suspended matter was filtered

https://doi.org/10.1021/acsomega.3c06090
ACS Omega 2023, 8, 38723−38732

off, and the solvent was distilled off in vacuum. The residue was triturated with EtOAc/diethyl ether (1:1), and the crystalline yellowish precipitate of **8b** was collected; yield 6.55 g (86%), mp 60−63 °C, IR (KBr) ν_{max}: 3361 (O−H), 3324 (O−H). ^{1}H NMR (400 MHz; D_2O, δ): 0.72 (s, 3H), 0.80 (s, 3H), 1.09 (t, J_t = 7.5 Hz, 3H), 2.29 (dq, J_q = 7.5 Hz, J_d = 15 Hz, 1H), 2.47−2.58 (m, 1H), 2.70 (dq, J_q = 7.5 Hz, J_d = 15 Hz, 1H), 2.82−2.92 (m, 1H), 3.71−3.95 (m, 4H). HRMS (EI/DFS) m/z: $[M]^+$ calcd for $C_{12}H_{19}{}^2H_4NO_3$ 233.1924; found 233.1922.

General Procedure of Hydrogen−Deuterium Exchange in Nitrones. A solution of nitrone **8a** or **8b** (1g) in 5% NaOD/D_2O (10 mL) was kept at ambient temperature for 20 days. The conversion was controlled by NMR spectroscopy. On the final step, the reaction stayed at 40 °C for another 5 days. After the exchange was finished, the reaction mixture was neutralized by dry CO_2 bubbled, and the solvent was distilled off in vacuum. To the residue, EtOAc (50−100 mL) was added and heated to the reflux. The precipitate obtained was filtered off; the solution was evaporated in vacuum to give nitrone **8c** or **8d** correspondingly.

2,2-Diethyl-5-(1-$^2H_2$)ethyl-3,4-bis((^{2}H)-hydroxymethyl)-3,4-dihydro-2*H*-(4-^{2}H)pyrrole 1-oxide (8c). ^{1}H NMR (300 MHz; 5% NaOD/D_2O, δ): 0.59 (t, J_t = 7.2 Hz, 3H), 0.68 (t, J_t = 7.3 Hz, 3H), 0.93 (s, 3H), 1.40−1.72 (m, 4H), 2.14 (dd, J_d = 5.3 Hz, J_d = 9 Hz, 1H), 3.25 (AB, J_{AB} = 10.8 Hz, 1H), 3.37−3.62 (m, 2H), 3.76 (AB, J_{AB} = 10.8 Hz, 1H).

2,2- Di(1-$^2H_4$)ethyl-5-(1-$^2H_2$)ethyl-3,4-bis((^{2}H)-hydroxymethyl)-3,4-dihydro-2*H*-(4-^{2}H)pyrrole 1-oxide (8d). ^{1}H NMR (300 MHz; 5% NaOD/D_2O, δ): 0.58 (s, 3H), 0.67 (s, 3H), 0.93 (s, 3H), 2.14 (dd, J_d = 5.3 Hz, J_d = 9 Hz, 1H), 3.25 (AB, J_{AB} = 10.8 Hz, 1H), 3.38−3.61 (m, 2H), 3.76 (AB, J_{AB} = 10.8 Hz, 1H).

2-Ethynyl-2,5,5-triethyl-3,4-bis(hydroxymethyl)-pyrrolidine-1-oxyls (10a and 12a−c). A solution of trimethylsilyl chloride (1.09 g, 10 mmol) in dry THF (10 mL) was added dropwise to a solution of nitrone **8a−d** (1 g, 4.37 mmol) and triethylamine (1.01 g, 10 mmol) in dry THF (35 mL) upon stirring in an ice bath. The reaction mixture was stirred at ambient temperature for 2 h. Then, the solvent was evaporated under reduced pressure, the residue was triturated with dry diethyl ether, and the precipitate was filtered off. The combined filtrate was concentrated under reduced pressure. Then, a solution of ethynylmagnesium bromide (0.6 M in THF, 44 mmol, 73 mL) was added in an argon atmosphere. The reaction mixture was kept at ambient temperature for 10 days. The mixture was quenched carefully with water until the formation of two phases. The organic layer was diluted with ether and separated, and the aqueous layer was extracted with EtOAc (15 mL × 3). The combined extract was evaporated under reduced pressure, the residue was dissolved in methanol (20 mL), and an aqueous solution of NaOH (0.05 g in 30 mL) was added to remove the protective groups. Then, catalytic amounts of methylene blue (2−3 mg) were added, and reaction mixture was bubbled with air for 12 h. Methanol was distilled off under reduced pressure, and the aqueous layer was acidified to pH 3−4 with 1 M H_2SO_4 and extracted with EtOAc (15 mL × 4). The organic extracts were collected and dried with Na_2SO_4, and the solvent was distilled off in vacuum. The residue was subjected to column chromatography on silica gel, eluent hexane/EtOAc (1:2), to give **10a** as yellow crystals; yield 0.98 g (88%), mp 112−114 °C, IR (KBr) ν_{max}: 3509 (O−H), 3444 (O−H), 3220 (C≡C−H), 2102 (C≡C). ^{1}H NMR (400 MHz; $CDCl_3/CD_3OD/CF_3COOH$, δ): 0.82 (t, J_t = 7.5 Hz, 3H), 0.84 (t, J_t = 7.5 Hz, 3H), 1.04 (t, J_t = 7.4 Hz, 3H), 1.67 (q, J_q = 7.4 Hz, 2H), 1.86−2.03 (m, 2H), 2.23 (m, 2H), 2.87 (s, 1H), 3.48−3.82 (m, 4H). HRMS (EI/DFS) m/z: $[M]^+$ calcd for $C_{14}H_{24}NO_3$ 254.1751; found 254.1753. Anal. Calcd for $C_{14}H_{24}NO_3$: C, 66.11; H, 9.51; N, 5.51. Found: C, 66.18; H, 9.65; N, 5.50. nitroxides **12a−c** were prepared using similar procedures from **8b−d**.

2-Ethynyl-2-(1-$^2H_4$)ethyl-5,5-diethyl-3,4-bis-(hydroxymethyl)-(3-^{2}H)pyrrolidine-1-oxyl (12a). Yellow crystals, yield 0.88 g (80%), IR (KBr) ν_{max}: 3506 (O−H), 3446 (O−H), 3224 (C≡C−H), 2102 (C≡C). ^{1}H NMR (400 MHz; $CDCl_3/CD_3OD/CF_3COOH$, δ): 0.83 (t, J_t = 7.5 Hz, 3H), 0.86 (t, J_t = 7.4 Hz, 3H), 1.04 (s, 3H), 1.68 (q, J_q = 7.4 Hz, 2H), 1.97 (q, J_q = 7.5 Hz, 2H), 2.26 (dd, J_d = 6.6; 3.7 Hz, 1H), 2.86 (s, 1H), 3.48−3.86 (m, 4H). HRMS (EI/DFS) m/z: $[M]^+$ calcd for $C_{14}H_{21}{}^2H_3NO_3$ 257.1955; found 257.1959.

2-Ethynyl-2-ethyl-5,5-di(1-$^2H_4$)ethyl-3,4-bis-(hydroxymethyl)-pyrrolidine-1-oxyl (12b). Yellow crystals, yield 0.95 g (86%), IR (KBr) ν_{max}: 3508 (O−H), 3444 (O−H), 3222 (C≡C−H), 2104 (C≡C). ^{1}H NMR (400 MHz; $CDCl_3/CD_3OD/CF_3COOH$, δ): 0.83 (s, 3H), 0.85 (s, 3H), 1.07 (t, J_t = 7.4 Hz, 3H), 1.83−2.06 (m, 2H), 2.26 (m, 1H), 2.85 (s, 1H), 3.48−3.87 (m, 4H). HRMS (EI/DFS) m/z: $[M]^+$ calcd for $C_{14}H_{20}{}^2H_4NO_3$ 258.2002; found 258.2000.

2-Ethynyl-2-(1-$^2H_4$)ethyl-5,5-di(1-$^2H_4$)ethyl-3,4-bis-(hydroxymethyl)-(3-^{2}H)pyrrolidine-1-oxyl (12c). Yellow crystals, yield 0.89 g (81%), IR (KBr) ν_{max}: 3506 (O−H), 3448 (O−H), 3222 (C≡C−H), 2104 (C≡C). ^{1}H NMR (400 MHz; $CDCl_3/CD_3OD/CF_3COOH$, δ): 0.78 (s, 3H), 0.80 (s, 3H), 1.00 (s, 3H), 2.20 (dd, J_d = 4.0; 6.2 Hz, 1H), 2.86 (s, 1H), 3.43−3.81 (m, 4H). HRMS (EI/DFS) m/z: $[M]^+$ calcd for $C_{14}H_{17}{}^2H_7NO_3$ 261.2206; found 261.2202.

General Procedure of Hydrogenation of Nitroxides 10a and 12a−c. A hydrogenation was performed in a reaction vessel equipped with a magnetic stirrer and a connection line to a gasometer filled with hydrogen/deuterium. Deuterium was prepared by dropwise addition of D_2O (3.5 mL) into a flask containing lithium foil (0.4−0.5 g) under the layer of absolute THF. A solution of nitroxide **10a** or **12a−c** (0.2 g) in THF (3 mL) was placed into the reaction vessel, the catalyst (Pd/C, 4%, 70 mg) was added to a solution, and the system was purged with hydrogen/deuterium and closed. The mixture was vigorously stirred until hydrogen absorption ceased, then the catalyst was filtered off and washed with THF, and slow stream of air was passed through the solution for 24 h. The solution was evaporated in vacuum, and the residue was subjected to column chromatography on silica gel, eluent hexane/EtOAc (1:1), to give yellow crystals **14** or **13a−d**.

2-((1-$^2H_2$-2-$^2H_2$)Ethyl)-2,5,5-triethyl-3,4-bis-(hydroxymethyl)-pyrrolidine-1-oxyl (13a). IR (KBr) ν_{max}: 3486 (O−H), 3446 (O−H). ^{1}H NMR (300 MHz; $CD_3OD/(CD_3)_2CO/CF_3COOH$, δ): 0.90−1.06 (m, 10H), 1.75−1.86 (m, 1H), 1.89−2.01 (m, 5H), 2.32 (m, 2H), 3.64−3.84 (m, 4H). HRMS (EI/DFS) m/z: $[M - H]^+$ calcd for $C_{14}H_{23}{}^2H_4NO_3$ 261.2237; found 261.2241.

2-((1-$^2H_2$-2-$^2H_2$)Ethyl)-2-(1-$^2H_2$)ethyl-5,5-diethyl-3,4-bis(hydroxymethyl)-(3-^{2}H)pyrrolidine-1-oxyl (13b). IR (KBr) ν_{max}: 3486 (O−H), 3452 (O−H). ^{1}H NMR (300 MHz; $CD_3OD/CDCl_3/CF_3COOH$, δ): 0.61−0.89 (m, 10H), 1.44−1.73 (m, 4H), 2.04 (m, 1H), 3.34−3.65 (m, 4H). HRMS

https://doi.org/10.1021/acsomega.3c06090
ACS Omega 2023, 8, 38723−38732

(EI/DFS) m/z: $[M]^+$ calcd for $C_{14}H_{21}{}^2H_7NO_3$ 265.2503; found 265.2505.

2-((1-$^2H_2$-2-$^2H_2$)Ethyl)-2-ethyl-5,5-di(1-$^2H_4$)ethyl-3,4-bis(hydroxymethyl)-pyrrolidine-1-oxyl (13c). IR (KBr) ν_{max}: 3486 (O−H), 3448 (O−H). ^1H NMR (500 MHz; $CD_3OD/CDCl_3/CF_3COOH$, δ): 0.90 (m, 1H), 0.93 (s, 3H), 0.96 (s, 3H), 0.98 (t, J_t = 7.5 Hz, 3H), 1.81−1.94 (m, 2H), 2.23 (m, 2H), 3.62 (m, 2H), 3.76 (m, 2H). HRMS (EI/DFS) m/z: $[M]^+$ calcd for $C_{14}H_{20}{}^2H_8NO_3$ 266.2566; found 266.2570.

2-((1-$^2H_2$-2-$^2H_2$)Ethyl)-2,5,5-tri(1-$^2H_6$)ethyl-3,4-bis-(hydroxymethyl)-(3-^2H)pyrrolidine-1-oxyl (13d). IR (KBr) ν_{max}: 3486 (O−H), 3448 (O−H). ^1H NMR (300 MHz; $CD_3OD/(CD_3)_2CO/CF_3COOH$, δ): 0.84−1.02 (m, 10H), 2.29 (m, 1H), 3.62−3.82 (m, 4H). HRMS (EI/DFS) m/z: $[M]^+$ calcd for $C_{14}H_{17}{}^2H_{11}NO_3$ 269.2754; found 269.2744.

2,5,5-Tri(1-$^2H_6$)ethyl-2-ethyl-3,4-bis(hydroxymethyl)-(3-^2H)pyrrolidine-1-oxyl (14). IR (KBr) ν_{max}: 3486 (O−H), 3446 (O−H). ^1H NMR (400 MHz; $CD_3OD/CDCl_3/CF_3COOH$, δ): 0.96 (s, 3H), 0.97 (t, J_t = 7.4 Hz, 3H), 0.99 (s, 6H), 1.72 (dq, J_d = 14.7 Hz, J_q = 7.4 Hz, 1H), 1.84 (dq, J_d = 14.7 Hz, J_q = 7.4 Hz, 1H), 2.25 (dd, J_d = 7.1 Hz, J_d = 3.9 Hz, 1H), 3.64 (d, J_d = 11.2 Hz, 1H), 3.64 (dd, J_d = 11.4 Hz, J_d = 7.1 Hz, 1H), 3.79 (d, J_d = 11.2 Hz, 1H), 3.79 (dd, J_d = 11.4 Hz, J_d = 3.9 Hz, 1H). HRMS (EI/DFS) m/z: $[M]^+$ calcd for $C_{14}H_{21}{}^2H_7NO_3$ 265.2503; found 265.2502.

CW EPR. The X-band EPR spectra were obtained in diluted and oxygen-free aqueous solutions at room temperature at concentrations of 10^{-4} M on a Bruker X-band (9 GHz) spectrometer Elexys E540. Experimental CW EPR settings were as follows: microwave power, 2.0 mW; modulation frequency, 100 kHz; modulation amplitude, 0.03 mT; time constant, 20 ms; sweep time, 21 s; number of points, 1024; number of scans, 1. For determining the isotropic g-values (g_{iso}), we recorded the X-band CW EPR spectra of mixtures of the investigated radicals with Tempo. The simulations of the solution EPR lines were carried out using different modes (fast motion model) in the software package EasySpin, which is available at www.easyspin.org.

Calculations. The geometry of conformations of the nitroxides was obtained from X-ray crystallography data (CCDC 1811119; CCDC 2209672) for **1a−c** and **5** and by systematic rotor search at the MMFF94 level in the Avogadro program[23] for corresponding ketones that form when NO is replaced by CO.

Following optimization was performed at the UB3LYP/def2-TZVP level.[24] The isotropic hyperfine splitting (a_{iso}) constants were calculated as isotropic Fermi contact couplings at the same level of theory.[25] The influence of a solvent on the a_{iso} constants was not taken into account. The results of the UB3LYP calculation did not suffer from the spin contamination effect; the expectation value of S^2 was within 0.754 and 0.755 for radicals. All calculations were performed with the ORCA 5.0.3[26] suite of programs with default settings. NBO analysis was performed with the NBO 7.0.10 program.[27] Visualization of the calculation results was performed with the ChemCraft program (https://www.chemcraftprog.com).

■ ASSOCIATED CONTENT

Supporting Information

The Supporting Information is available free of charge at https://pubs.acs.org/doi/10.1021/acsomega.3c06090.

Copies of the ^1H NMR, IR, and HRMS spectra of compounds and DFT calculations data (PDF)

■ AUTHOR INFORMATION

Corresponding Author

Yuliya F. Polienko − *N.N. Vorozhtsov Novosibirsk Institute of Organic Chemistry SB RAS, Novosibirsk 630090, Russia;* orcid.org/0000-0002-1770-1968; Email: polienko@nioch.nsc.ru

Authors

Sergey A. Dobrynin − *N.N. Vorozhtsov Novosibirsk Institute of Organic Chemistry SB RAS, Novosibirsk 630090, Russia*

Konstantin A. Lomanovich − *N.N. Vorozhtsov Novosibirsk Institute of Organic Chemistry SB RAS, Novosibirsk 630090, Russia*

Anastasiya O. Brovko − *N.N. Vorozhtsov Novosibirsk Institute of Organic Chemistry SB RAS, Novosibirsk 630090, Russia; Department of Natural Sciences, Novosibirsk State University, Novosibirsk 630090, Russia*

Elena G. Bagryanskaya − *N.N. Vorozhtsov Novosibirsk Institute of Organic Chemistry SB RAS, Novosibirsk 630090, Russia;* orcid.org/0000-0003-0057-383X

Igor A. Kirilyuk − *N.N. Vorozhtsov Novosibirsk Institute of Organic Chemistry SB RAS, Novosibirsk 630090, Russia;* orcid.org/0000-0001-6033-0368

Complete contact information is available at: https://pubs.acs.org/10.1021/acsomega.3c06090

Notes

The authors declare no competing financial interest.

■ ACKNOWLEDGMENTS

This work was supported by the Russian Science Foundation (grant number 22-73-00098). We thank the Multi-Access Chemical Research Center SB RAS for spectral and analytical measurements.

■ REFERENCES

(1) Ouari, O.; Gigmes, D.; Ouari, O.; Gigmes, D. *nitroxides: Synthesis, Properties and Applications*; Royal Society of Chemistry, 2021.

(2) Kokorin, A. I. nitroxides: Theory, Experiment and Applications. *InTech* **2012**, DOI: 10.5772/2887.

(3) Likhtenshtein, G. I.; Yamauchi, J.; Nakatsuji, S.; Smirnov, A.; Tamura, R. nitroxides: Applications in Chemistry, Biomedicine, and Material Science; Wiley-VCH Verlag GmbH & Co. *KGaA* **2008**.

(4) Paletta, J. T.; Pink, M.; Foley, B.; Rajca, S.; Rajca, A. Synthesis and reduction kinetics of sterically shielded pyrrolidine nitroxides. *Org. Lett.* **2012**, *14*, 5322−5325.

(5) Jagtap, A. P.; Krstic, I.; Kunjir, N. C.; Hänsel, R.; Prisner, T. F.; Sigurdsson, S. T. Sterically shielded spin labels for in-cell EPR spectroscopy: Analysis of stability in reducing environment. *Free Radic. Res.* **2015**, *49*, 78−85.

(6) Ovcherenko, S. S.; Chinak, O. A.; Chechushkov, A. V.; Dobrynin, S. A.; Kirilyuk, I. A.; Krumkacheva, O. A.; Richter, V. A.; Bagryanskaya, E. G. Uptake of cell-penetrating peptide rl2 by human lung cancer cells: Monitoring by electron paramagnetic resonance and confocal laser scanning microscopy. *Molecules* **2021**, *26*, 5442.

(7) Dobrynin, S. A.; Glazachev, Y. I.; Gatilov, Y. V.; Chernyak, E. I.; Salnikov, G. E.; Kirilyuk, I. A. Synthesis of 3,4-Bis(hydroxymethyl)-2,2,5,5-tetraethylpyrrolidin-1-oxyl via 1,3-Dipolar Cycloaddition of Azomethine Ylide to Activated Alkene. *J. Org. Chem.* **2018**, *83*, 5392−5397.

(8) Dobrynin, S. A.; Usatov, M. S.; Zhurko, I. F.; Morozov, D. A.; Polienko, Y. F.; Glazachev, Y. I.; Parkhomenko, D. A.; Tyumentsev, M. A.; Gatilov, Y. V.; Chernyak, E. I.; Bagryanskaya, E. G.; Kirilyuk, I. A. A Simple Method of Synthesis of 3-Carboxy-2,2,5,5-Tetraethylpyrrolidine-1-oxyl and Preparation of Reduction-Resistant Spin Labels and Probes of pyrrolidine Series. *Molecules* **2021**, *26*, 5761.
(9) Zhurko, I. F.; Dobrynin, S.; Gorodetskii, A. A.; Glazachev, Y. I.; Rybalova, T. V.; Chernyak, E. I.; Asanbaeva, N.; Bagryanskaya, E. G.; Kirilyuk, I. A. 2-Butyl-2-tert-butyl-5,5-diethylpyrrolidine-1-oxyls: Synthesis and properties. *Molecules* **2020**, *25*, 1−17.
(10) Rančić, A.; Babić, N.; Orio, M.; Peyrot, F. Structural Features Governing the Metabolic Stability of Tetraethyl-Substituted nitroxides in Rat Liver Microsomes. *Antioxidants* **2023**, *12*, 402.
(11) Dobrynin, S. A.; Gulman, M. M.; Morozov, D. A.; Zhurko, I. F.; Taratayko, A. I.; Sotnikova, Y. S.; Glazachev, Y. I.; Gatilov, Y. V.; Kirilyuk, I. A. Synthesis of sterically shielded nitroxides using the reaction of nitrones with alkynylmagnesium bromides. *Molecules* **2022**, *27*, 7626.
(12) Eaton, S. S.; van Willigen, H.; Heining, M. J.; Eaton, G. R. ENDOR measurements of long-range hyperfine coupling in a nitroxyl radical. *J. Magn. Reson.* **1980**, *38*, 325−330.
(13) Heining, M. J.; Eaton, G. R.; Eaton, S. S. Electron paramagnetic resonance as a probe of conformational flexibility in cyclic alkanes. *Appl. Spectrosc.* **1980**, *34* (3), 268−275.
(14) Bobko, A. A.; Kirilyuk, I. A.; Gritsan, N. P.; Polovyanenko, D. N.; Grigor'ev, I. A.; Khramtsov, V. V.; Bagryanskaya, E. G. EPR and Quantum Chemical Studies of the pH-sensitive Imidazoline and imidazolidine nitroxides with Bulky Substituents. *Appl. Magn. Reson.* **2010**, *39*, 437−451.
(15) Taratayko, A. I.; Trakhinina, S. Yu.; Lomanovich, K. A.; Kirilyuk, I. A. A novel method for the sterically shielded pyrroline nitroxides synthesis using donor-acceptor cyclopropanes. *Tetrahedron Lett.* **2023**, *123*, No. 154546.
(16) Hyodo, F.; Murugesan, R.; Matsumoto, K.; Hyodo, E.; Subramanian, S.; Mitchell, J. B.; Krishna, M. C. Monitoring redox-sensitive paramagnetic contrast agent by EPRI. *OMRI and MRI. J. Magn. Reson.* **2008**, *190* (1), 105−112.
(17) Jebaraj, D. D.; Utsumi, H.; Benial, A. M. F. Electron spin resonance studies on deuterated nitroxyl spin probes used in Overhauser-enhanced magnetic resonance imaging. *Magn. Reson. Chem.* **2017**, *55* (8), 700−705.
(18) Fehling, P.; Buckenmaier, K.; Dobrynin, S. A.; Morozov, D. A.; Polienko, Yu.F.; Khoroshunova, Yu.V.; Borozdina, Yu.; Mayer, P.; Engelmann, J.; Scheffler, K.; Angelovski, G.; Kirilyuk, I. A. The effects of nitroxide structure upon 1H Overhauser dynamic nuclear polarization efficacy at ultralow-field. *J. Chem. Phys.* **2021**, *155* (14), 144203.
(19) Elsworth, M.; Lamchen, J. F. Nitrones: part X1 tautomerism in cyclic nitrones. *S. Afr. J. Chem.* **1970**, *23* (2), 61−70.
(20) Fraser, R. R.; Champagne, P. J. Highly stereoselective H-D exchange of diastereotopic protons in 4',1"-dimethyl-1,2,3,4-dibenzylcyclohepta-1,3-diene-6-one. *Can. J. Chem.* **1976**, *54* (23), 3809−3811.
(21) Saracino, G. A. A.; Tedeschi, A.; D'Errico, G.; Improta, R.; Franco, L.; Ruzzi, M.; Corvaia, C.; Barone, V. Solvent Polarity and pH Effects on the Magnetic Properties of Ionizable nitroxide Radicals: A Combined Computational and Experimental Study of 2,2,5,5-Tetramethyl-3-carboxypyrrolidine and 2,2,6,6-Tetramethyl-4-carboxypiperidine nitroxides. *J. Phys. Chem. A* **2002**, *106* (44), 10700−10706.
(22) Hermosilla, L.; de la Vega, J. M.; Sieiro, C.; Calle, P. DFT Calculations of Isotropic Hyperfine Coupling Constants of Nitrogen Aromatic Radicals: The Challenge of nitroxide Radicals. *J. g. Theory Comput.* **2011**, *7* (1), 169−179.
(23) Hanwell, M. D.; Curtis, D. E.; Lonie, D. C.; Vandermeersch, T.; Zurek, E.; Hutchison, G. R. Avogadro: an advanced semantic chemical editor, visualization, and analysis platform. *J. ChemInform.* **2012**, *4* (1), 17.
(24) Lee, C.; Yang, W.; Parr, R. G. Development of the Colle-Salvetti correlation-energy formula into a functional of the electron density. *Phys. Rev. B* **1988**, *37* (2), 785.
(25) Munzarová, M. L. DFT calculations of EPR hyperfine coupling tensors. In *Calculation of NMR and EPR Parameters: Theory and Applications*; Kaupp, M., Bühl, M., Malkin, V. G., Eds.; Wiley-VCH Verlag GmbH & Co. KGaA, 2004; pp 461−482.
(26) Neese, F.; Wennmohs, F.; Becker, U.; Riplinger, C. The ORCA quantum chemistry program package. *J. Chem. Phys.* **2020**, *152* (22), 224108.
(27) NBO 7.0. Glendening, E. D.; Badenhoop, J. K.; Reed, A. E.; Carpenter, J. E.; Bohmann, J. A.; Morales, C. M.; Karafiloglou, P.; Landis, C. R.; Weinhold, F. Theoretical Chemistry Institute, University of Wisconsin, Madison, WI (2018).

https://doi.org/10.1021/acsomega.3c06090
ACS Omega 2023, 8, 38723−38732